DOI 10.4430/bgo00424

Intensified flows in free modes

F. Crisciani[1] and R. Mosetti[2]

[1] Former Research Executive, CNR-ISMAR, Trieste, Italy
[2] Former Research Director, National Institute of Oceanography and Applied Geophysics - OGS, Trieste, Italy

(Received: 21 February 2023; accepted: 15 May 2023; published online: 25 August 2023)

ABSTRACT In the framework of stable free modes, a criterion is derived for the localisation in latitude of the intensified sector of the mode, i.e. northwards, southwards, or equally distributed in the north and south. The criterion is based on the sign taken by the inverse of the total vorticity at the middle latitude of the reference basin, and resorts to the necessarily westward orientation of an unforced current according to one of Greenspan's theorems. Some solutions, also of non-linear modes, elucidate the result.

Key words: free modes, mass transport, intensified flows.

1. Introduction

Free modes have the unfortunate characteristic of being devoid of a well-established phenomenological counterpart in the real ocean. The circulation, resulting on the beta plane, takes place in the absence of forcing and dissipation. In a sense, free modes are a kind of 'ground state' of the adiabatic ocean in steady motion, under the effect of Coriolis acceleration and its meridional gradient. Relative vorticity is also requested for having closed streamlines in a bounded basin. Wind stress yields equations that are more suited in dealing with processes of the real ocean. It is important to underline that free modes also emerge in statistical fluid mechanics in the form of mean field equations and, again, that they are a kind of ground state for steady ocean circulation at middle latitude (Bouchet and Venaille, 2012). A free mode is governed by the conservation of the total vorticity, i.e. relative plus planetary, and an equation in close form is easily achieved in the framework of the quasi-geostrophic context. The fact that this equation exhibits the dependence of the stream function, on the total vorticity in a widely arbitrary form, is a critical point, which makes multiple solutions feasible.

In a seminal paper by Fofonoff (1954), often cited in textbooks (Krauss, 1973; Hendershott, 1987; Pedlosky, 1987, 1996; Vallis, 2006), this dependence is taken linear only to dribble mathematical intricacies. Fofonoff's solution shows the formation of an intensified current in the proximity of one of the zonal boundaries. However, the addition of a constant to the total vorticity can transfer the intensification from one zonal boundary to the other or, otherwise, eliminate the asymmetry caused by it. All this can be easily explained in an elementary way, however, if the linear dependence of the stream function on the total vorticity is released, the localisation of the intensified current (if any) no longer has an obvious explanation, and the mechanism of adding a constant no longer works. At this point, the question, namely on how the localisation of the intensification is determined, arises.

This is just the central question, which will be answered in this work. Some preliminary aspects, necessary to frame the problem, are considered in section 2. Section 3 points out two

© 2023 - OGS

symmetric properties of the flow patterns in free modes, which are strictly related to the mass transport in the proximity of the basin boundaries. The relationship between transport and total vorticity is inferred in section 4, where the localisation of the intensified zonal transport is explicitly determined by the total vorticity. Section 5 analyses two non-linear free modes in an elongated basin to show how the method inferred in section 4 works in specific cases.

2. Framework

All the foregoing quantities are dimensionless and of the order of unit, unless otherwise specified. Considering the fluid domain included in a certain beta plane as:

$$D = [(x, y): -\lambda \leq x \leq \lambda,\ 0 \leq y \leq 1] \tag{1}$$

inside *D* a constant-density fluid is in inertial and steady motion with velocity **u**. So, potential vorticity Π of each fluid column is conserved according to the equation:

$$\mathbf{u} \cdot \nabla\ \Pi = 0 . \tag{2}$$

In Eq. 2:

$$\Pi = \hat{\mathbf{k}} \cdot rot\ \mathbf{u} + \beta y . \tag{3}$$

The unit vector $\hat{\mathbf{k}}$ is normal to the beta plane to which *D* belongs, and *β* is the (dimensionless) planetary vorticity gradient. The assumed geophysical nature of the circulation implies:

$$\beta >> 1 . \tag{4}$$

The geostrophic formulation of Eq. 2 with Eq. 3 yields a useful and compact governing equation. In fact, if **u** is geostrophic, it can be expressed by means of a stream function $\psi(x, y)$ such as:

$$\mathbf{u} = \hat{\mathbf{k}} \times \nabla \psi \tag{5}$$

and, hence:

$$\hat{\mathbf{k}} \cdot rot\ \mathbf{u} = \nabla^2 \psi . \tag{6}$$

By resorting to the notation of the Jacobian determinant:

$$J(\psi,\ q) = \frac{\partial \psi}{\partial x}\frac{\partial q}{\partial y} - \frac{\partial q}{\partial x}\frac{\partial \psi}{\partial y}$$

where $\psi(x, y)$ and $q(x, y)$ are differentiable fields[1], substitution of Eqs. 5 and 6 into Eq. 2 results, after little algebra, in the equation:

[1] In the present context ψ is the stream function, while $q = \nabla^2\psi + \beta y$.

$$J\left(\psi,\ \nabla^2\psi+\beta y\right)=0\,. \tag{7}$$

Eq. 7 is satisfied by any functional relationship between stream function ψ and potential vorticity $\nabla^2\psi + \beta y$ of the kind $F(\psi, \nabla^2\psi + \beta y) = 0$ that is usually written as:

$$\nabla^2\psi+\beta y=\mathsf{Q}\left(\psi\right) \tag{8}$$

where Q is a smooth and differentiable function of its argument. According to Eq. 4, the left side of Eq. 8 is in the order of max $\{O(\nabla^2\psi), O(\beta y)\}$, that is in the order of β, and, therefore, the left and right sides of Eq. 8 balance each other, provided that Q is of the same order. This suggests setting:

$$\mathsf{Q}\left(\psi\right)=\beta\, Q\left(\psi\right) \tag{9}$$

where Q is of order one. Then, substitution of Eq. 9 into Eq. 8 and the subsequent division by β yields:

$$\beta^{-1}\nabla^2\psi+y=Q\left(\psi\right). \tag{10}$$

Factor β^{-1}, appearing in Eq. 10, is the square ratio between the so-called inertial boundary layer width δ_I and horizontal length scale L [see, e.g. Pedlosky (1987)]. In terms of δ_I and L, Eq. 10 takes the final form:

$$\left(\delta_I/L\right)^2\nabla^2\psi+y=Q\left(\psi\right) \tag{11}$$

where

$$\left(\delta_I/L\right)^2<<1 \tag{12}$$

is in accordance with Eq. 4. Definite values of δ_I/L are not strictly binding in the following investigation. Conversely, the lack of observational evidence of free modes prevents from having precise indications in this regard. Regarding $Q(\psi)$, assumption:

$$Q_\psi>0 \tag{13}$$

is in order (the subscript means differentiation with respect to ψ). Inequality in Eq. 13 restricts the class of the modes that will be taken into account, but it is essential for investigating the characteristic intensification of the modes selected by Eq. 13. Modes in which $Q_\psi < 0$ [e.g. Moro (1987) and Pedlosky (2016)] are candidates to instability and are not amenable to the analysis treated here. The inertial nature of a free mode implies that its boundary condition is purely kinematic. Let $\hat{\mathbf{n}}$ be the local unit vector of the (x, y) plane normal to ∂D. As Eq. 1 is simply connected, the condition of no mass-flux across ∂D, that is:

$$\hat{\mathbf{n}} \cdot \mathbf{u} = 0 \ \forall (x,y) \in \partial D$$

can be re-stated, by means of Eq. 5, in the form:

$$\psi = 0 \ \forall (x,y) \in D. \tag{14}$$

To summarise, free modes to be explored are governed by Eq. 11 with Eq. 14, and further subject to Eqs. 12 and 13. The model solution of Eqs. 11 to 14 is non-zero, unique and non-linearly stable according to Blumen (1968). Wherever relative vorticity satisfies inequality $\nabla^2\psi << (L\ \delta_I)^2$, the first term of Eq. 11 is smaller than the unit and Eq. 11 simplifies into:

$$y = Q(\psi). \tag{15}$$

Since Eq. 15 is not able to satisfy Eq. 14, nor is it valid in boundary layers, it is re-written more properly in terms of the new variable ψ_{int}:

$$y = Q(\psi_{\text{int}}). \tag{16}$$

Owing to Eq. 13, Eq. 15 can be inverted to make ψ_{int} explicit:

$$\psi_{\text{int}} = Q^{-1}(y). \tag{17}$$

For future purposes, interior D_{int} of Eq. 1 is defined as the portion of D where the restriction of ψ into D_{int} is given by Eq. 17. An important consequence is that the interior current, i.e. u_{int}, is necessarily westwards. In fact, differentiation of Eq. 15, with respect to y and Eq. 13, shows that:

$$u_{\text{int}} = -Q_{\psi}^{-1}(\psi_{\text{int}}) \ < 0. \tag{18}$$

Eq. 18 is a special case of Greenspan's theorem (Greenspan, 1962).

3. Symmetry and asymmetry of flow patterns in free modes

Symmetry and asymmetry of flow patterns are the inspiring features that lead to the results inferred in the next section. The general method, already used elsewhere (Crisciani and Badin, 2014; Crisciani and Mosetti, 2021, 2022), consists in expressing the stream function as the sum of virtual terms having definite symmetric/anti-symmetric properties under the transformation of D into itself, and that influence the original stream function. This fact poses the question of whether and how $Q(\psi)$ determines such properties.

The symmetric (ψ_s) and anti-symmetric (ψ_a) components of the solution of Eqs. 11 to 14 under the mirror reflection:

$$(x,y) \mapsto (-x,y) \tag{19}$$

of D into itself are

$$\psi_s = \frac{1}{2}\left[\psi\left(x,y\right)+\psi\left(-x,y\right)\right],\ \psi_a = \frac{1}{2}\left[\psi\left(x,y\right)-\psi\left(-x,y\right)\right]. \tag{20}$$

Positions in Eq. 20 yield:

$$\psi = \psi_s + \psi_a,\ \psi_s\left(-x,y\right) = \psi_s\left(x,y\right),\ \psi_a\left(-x,y\right) = -\psi_a\left(x,y\right). \tag{21}$$

Moreover, the invariance:

$$\nabla^2 \mapsto \nabla^2 \tag{22}$$

under Eq. 19 is immediate. The boundary condition in Eq. 14 extends, separately and with the same form, also to ψ_s and to ψ_a. With the first part of Eq. 21 substituted into Eq. 11, the vorticity equation takes the form:

$$\left(\delta_I / L\right)^2 \nabla^2\left(\psi_s + \psi_a\right) + y = Q\left(\psi_s + \psi_a\right). \tag{23}$$

Transformation in Eq. 19 applied to Eq. 23 changes it according to the second and third parts of Eq. 21 and Eq. 22, that is:

$$\left(\delta_I / L\right)^2 \nabla^2\left(\psi_s - \psi_a\right) + y = Q\left(\psi_s - \psi_a\right). \tag{24}$$

Subtraction of Eq. 24 from Eq. 23 with the aid of the Lagrange theorem gives:

$$\left(\delta_I / L\right)^2 \nabla^2 \psi_a = Q_\psi\left(\xi\right)\psi_a \tag{25}$$

where ξ is a function of ψ_s and ψ_a. Multiplication of Eq. 25 by ψ_a, and the subsequent integration on D with the aid of the divergence theorem and Eq. 14, results in the equation:

$$-\left(\delta_I / L\right)^2 \int_D \left|\nabla \psi_a\right|^2 dxdy = \int_D Q_\psi\left(\xi\right)\ \psi_a^2 dxdy. \tag{26}$$

Given that the left side of Eq. 26 is not positive, while the right one is not negative (recall Eq. 13), this equation implies $\psi_a = 0$. Therefore:

$$\psi\left(x,y\right) = \psi\left(-x,y\right). \tag{27}$$

The mirror symmetry in Eq. 27, of the solution of the problem in Eqs. 11 to 14, is so proved. Note that Eq. 27 critically depends on Eq. 13, but it is independent from any special value of δ_I/L.

Once again consider the solution of the problem in Eqs. 11 to 14. The symmetric (ψ^s) and anti-symmetric (ψ^a) virtual components of ψ under the transformation:

$$\left(x,y\right)\mapsto\left(x,1-y\right) \tag{28}$$

of *D* into itself are:

$$\psi^{s}=\frac{1}{2}\left[\psi\left(x,y\right)+\psi\left(x,1-y\right)\right],\ \psi^{a}=\frac{1}{2}\left[\psi\left(x,y\right)-\psi\left(x,1-y\right)\right]. \tag{29}$$

Positions in Eq. 29 yield:

$$\psi=\psi^{s}+\psi^{a},\ \psi^{s}\left(x,1-y\right)=\psi^{s}\left(x,y\right),\ \psi^{a}\left(x,1-y\right)=-\psi^{a}\left(x,y\right). \tag{30}$$

The invariance:

$$\nabla^{2}\mapsto\nabla^{2} \tag{31}$$

under Eq. 28 is immediate. Substitution of the first part of Eq. 30 into Eq. 11 gives:

$$\left(\delta_{I}/L\right)^{2}\nabla^{2}\left(\psi^{s}+\psi^{a}\right)+y=Q\left(\psi^{s}+\psi^{a}\right) \tag{32}$$

and application of Eqs. 28 to 32, with the transformation rules in Eqs. 30 and 31, yields:

$$\left(\delta_{I}/L\right)^{2}\nabla^{2}\left(\psi^{s}-\psi^{a}\right)+1-y=Q\left(\psi^{s}-\psi^{a}\right). \tag{33}$$

Addition of Eq. 32 with Eq. 33 results in the equation:

$$2\left(\delta_{I}/L\right)^{2}\nabla^{2}\psi^{s}+1=Q\left(\psi^{s}+\psi^{a}\right)+Q\left(\psi^{s}-\psi^{a}\right). \tag{34}$$

Assume now:

$$\psi^{a}=0 \tag{35}$$

Eq. 35 presupposes $\psi=\psi^{s}\neq 0$. Due to Eq. 35, Eq. 34 becomes:

$$\left(\delta_{I}/L\right)^{2}\nabla^{2}\psi+1/2=Q\left(\psi\right). \tag{36}$$

Differentiation of Eq. 36 with respect to *y* gives:

$$\left(\delta_{I}/L\right)^{2}\nabla^{2}\psi_{y}=Q_{\psi}\psi_{y} \tag{37}$$

while, under the same differentiation, Eq. 11 takes the form:

$$\left(\delta_{I}/L\right)^{2}\nabla^{2}\psi_{y}+1=Q_{\psi}\psi_{y}. \tag{38}$$

The comparison between Eqs. 37 and 38 shows absurd 1 = 0. Therefore, assumption in Eq. 35 must be rejected. Hence, according to the second part of Eq. 28:

$$\psi\left(x,y\right)\neq\psi\left(x,1-y\right). \tag{39}$$

Asymmetry in Eq. 39 is better highlighted by the translation $(x, y)\to(x, 1/2 - y)$ of the frame of reference that transforms in Eq. 39 into:

$$\psi\left(x,\ 1/2-y\right)\neq\left(x,\ 1/2+y\right). \tag{40}$$

Inequalities in Eqs. 39 and 40 only rely on Eq. 11, while Eqs. 12 to 14 play no role in the derivation. Asymmetry in Eqs. 39 or 49 is the origin of northward or southward intensification.

4. Method and results

Relative flow intensification can be described by comparing mass transport in different regions of the fluid domain, and explained on the basis of the underlying symmetry properties of the transport. The westward intensification of the wind-driven circulation in subtropical gyres is an example (see e.g. Crisciani and Mosetti, 2021). In the case of the model represented by Eqs. 11 to 14, the main question, already anticipated in the introduction, is how $Q(\psi)$ determines the localisation of the intensified transport into D. For instance, the patterns of the well-known Fofonoff mode, evaluated for $Q(\psi) = \psi$, $Q(\psi) = \psi + 1$, $Q(\psi) = \psi + 1/2$ and illustrated in Fig. 1, show different locations of the intensified current. Obviously, the answer to the above question should cover a class of $Q(\psi)$ functions as wide as possible.

Meridional mass transports $\mathbf{M}_W = M_W\hat{\mathbf{j}}$ and $\mathbf{M}_E = M_E\hat{\mathbf{j}}$ take place in the westernmost (subscript W) and easternmost (subscript E) areas of the basin, and are given by:

$$\begin{aligned} M_W &= \int_{\lambda-X}^{\lambda} v\,dx = \int_{\lambda-X}^{\lambda} \frac{\partial\psi}{\partial x}dx = -\psi\left(\lambda-X,y\right) \\ M_E &= \int_{-\lambda}^{-\lambda+X} v\,dx = \int_{-\lambda}^{-\lambda+X} \frac{\partial\psi}{\partial x}dx = \psi\left(-\lambda+X,y\right). \end{aligned} \tag{41}$$

The streamlines lose their zonal trend only in the proximity of the meridional boundaries where they bend over to form close patterns, so a reasonable (though inessential) estimate of width X is $\delta_I/L \approx X$ ($<<\lambda$). Given that free modes satisfy symmetry in Eq. 27, Eq. 41 implies at any latitude:

$$\mathbf{M}_E+\mathbf{M}_W=0. \tag{42}$$

Thus, there is no preferential intensification, regardless of what $Q(\psi)$ may be.

In a somewhat different way, the zonal mass transport can be conveniently explored by introducing partition $\mathbf{M} = \mathbf{M}_S + \mathbf{M}_0 + \mathbf{M}_N$ where:

$$\mathbf{M}_S=M_S\hat{\mathbf{i}},\ \mathbf{M}_0=M_0\hat{\mathbf{i}},\ \mathbf{M}_N=M_N\hat{\mathbf{i}}$$

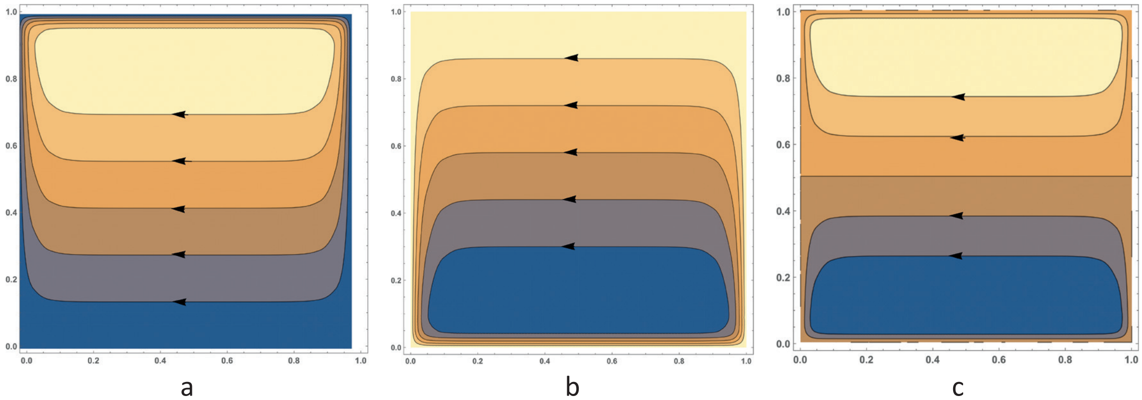

Fig. 1 - Some classic patterns of the Fofonoff mode in square domain $(0 \le x \le 1) \times (0 \le y \le 1)$. Panel a corresponds to $Q(\psi) = \psi$, panel b to $Q(\psi) = \psi + 1$, and panel c to $Q(\psi) = \psi + 1/2$.

and

$$M_S = \int_0^Y u\,dy = -\int_0^Y \frac{\partial\psi}{\partial y}dy = -\psi(x,Y)$$
$$M_0 = \int_Y^{1-Y} u\,dy = -\int_Y^{1-Y} \frac{\partial\psi}{\partial y}dy = -\psi(x,1-Y) + \psi(x,Y) \qquad (43)$$
$$M_N = \int_{1-Y}^{1} u\,dy = -\int_{1-Y}^{1} \frac{\partial\psi}{\partial y}dy = \psi(x,1-Y).$$

$\mathbf{M}_S$ (subscript S stands for south) is the zonal mass transport through the cross section extended from $y = 0$ to $y = Y$ ($Y < 1/2$), and $\mathbf{M}_N$ (subscript N stands for north) is the zonal mass transport through the cross section extended from $y = 1 - Y$ to $y = 1$. Finally, mass conservation yields $\mathbf{M}_0 = -(\mathbf{M}_S + \mathbf{M}_N)$. Thus, Y is the width cross section of both M_S and M_N. The further step forward is hypothesis:

$$(x,Y) \in D_{\text{int}} \text{ and } (x,1-Y) \in D_{\text{int}}. \qquad (44)$$

In Eq. 44, (x, Y) and $(x, 1 - Y)$ are the arguments of the stream function appearing in Eq. 43. Therefore, owing to Eqs. 44 and 17:

$$\psi(x,Y) = \psi_{\text{int}}(Y) = Q^{-1}(Y),\ \psi(x,1-Y) = \psi_{\text{int}}(1-Y) = Q^{-1}(1-Y). \qquad (45)$$

Substitution of Eq. 43 into Eq. 45 allows to express the zonal mass transport components in terms of the inverse of $Q(\psi)$, that is to say:

$$M_S = -Q^{-1}(Y),\ M_0 = Q^{-1}(Y) - Q^{-1}(1-Y),\ M_N = Q^{-1}(1-Y). \qquad (46)$$

Differential inequality in Eq. 13 implies the algebraic inequality:

$$Q^{-1}\left(1-Y\right)>Q^{-1}\left(Y\right) \tag{47}$$

that will soon be useful. Using the first part of Eq. 30, results in $M_S = -\psi^s(x, Y) - \psi^a(x, Y)$, so the first part of Eq. 46 takes the form:

$$\psi^s\left(x,Y\right)+\psi^a\left(x,Y\right)=Q^{-1}\left(Y\right). \tag{48}$$

Then, application of Eqs. 28 to 48 gives:

$$\psi^s\left(x,Y\right)-\psi^a\left(x,Y\right)=Q^{-1}\left(1-Y\right).$$

Hence, the following are found separately:

$$\psi^s\left(x,Y\right)=\frac{1}{2}\left[Q^{-1}\left(Y\right)+Q^{-1}\left(1-Y\right)\right]$$
$$\psi^a\left(x,Y\right)=\frac{1}{2}\left[Q^{-1}\left(Y\right)-Q^{-1}\left(1-Y\right)\right].$$

Thus, mass transport M_S can be written as the sum of a symmetric term (M_S^s) plus an anti-symmetric one (M_S^a), for example, $M_S = M_S^s + M_S^a$, where:

$$M_S^s=-\frac{1}{2}\left[Q^{-1}\left(Y\right)+Q^{-1}\left(1-Y\right)\right],\ M_S^a=\frac{1}{2}\left[Q^{-1}\left(1-Y\right)-Q^{-1}\left(Y\right)\right]. \tag{49}$$

The partition into symmetric and anti-symmetric terms, analogous to Eq. 49, can be extended to remaining Eq. 46. On the whole, the resulting equations are:

$$\begin{aligned}
M_N^s &= -M_S^s = \frac{1}{2}\left[Q^{-1}\left(Y\right)+Q^{-1}\left(1-Y\right)\right]\\
M_N^a &= M_S^a = \frac{1}{2}\left[Q^{-1}\left(1-Y\right)-Q^{-1}\left(Y\right)\right]\\
M_0^s &= 0\\
M_0^a &= Q^{-1}\left(Y\right)-Q^{-1}\left(1-Y\right)\ .
\end{aligned} \tag{50}$$

Eq. 50 provides the tool to explain the mechanism of intensification. First of all, Eq. 47 implies $M_0^a = M_0 < 0$, which is in accordance with the fact that $\mathbf{M}_0$ takes place into D_{int} where Eq. 18 holds. Then, anti-symmetric eastward mass transports $M_N^a = M_S^a > 0$ balance M_0^a by the formation of an anti-cyclonic circulation to the north ($1/2 < y < 1$) and a cyclonic one to the south ($0 < y < 1/2$). The fact that only M_N^s and M_S^s have no prefixed sign makes their role clear, in fact:

- if $M_N^s > 0$ ($M_S^s < 0$), then, $M_N = M_N^s + M_N^a > M_S^a$, while $M_S = M_S^s + M_S^a < M_S^a$, and, therefore, $M_N > M_S$. In other words, the mass transport along the northern boundary is intensified with respect to M_N^a, while that along the southern boundary is correspondingly weakened.

Alternatively,

- if $M_N^s < 0$ ($M_S^s > 0$), then, $M_N = M_N^s + M_N^a < M_S^a$, while $M_S = M_S^s + M_S^a > M_S^a$, and, therefore,

$M_S > M_N$. In this case, the mass transport along the northern boundary is correspondingly weakened with respect to M_N^a, while that along the southern boundary is intensified.

The above considerations show that the location of the intensification depends on the sign of $Q^{-1}(Y) + Q^{-1}(1-Y)$, which is positively correlated with that of M_N^s (and negatively with that of M_S^s), as the first part of Eq. 30 shows. To address this point, consider function $p(y)$ defined on $(0 \le y \le 1)$ by:

$$p(y)=\frac{1}{2}\left[Q^{-1}(y)+Q^{-1}(1-y)\right]. \tag{51}$$

Given that $p(1/2) = Q^{-1}(1/2)$ and $p(1/2 - y) = p(1/2 + y)$, $Q^{-1}(1/2)$ turns out to be an extremum of $p(y)$. Consequently:

- if $Q^{-1}(1/2) > 0$, then, $p(y) > 0 \;\; \forall y \in I_1 = (1/2 - y_1 < y < 1/2 + y_1)$ for a suitable y_1. Thus, $p(Y) = p(1-Y) > 0 \;\; \forall Y \in I_1$. Under hypothesis in Eq. 44, function $p(Y)$ can be identified with M_N^s, whence $M_N^s > 0$ (and, consequently, $M_S^s < 0$). Therefore, as above explained:

$$Q^{-1}(1/2)>0 \Rightarrow M_N > 0 \tag{52}$$

and, consequently, relative intensification is northwards and $\mathbf{M}_N$ is eastwards.

Alternatively,

- if $Q^{-1}(1/2) < 0$, then, $p(y) < 0 \;\; \forall y \in I_2 = (1/2 - y_2 < y < 1/2 + y_2)$ for a suitable y_2. Thus, $p(Y) = p(1 - Y) < 0 \;\; \forall Y \in I_2$. Under hypothesis in Eq. 44, function $p(Y)$ can be identified with $-M_S^s$, whence $M_S^s > 0$ (and, consequently, $M_N^s < 0$). Therefore, as above explained:

$$Q^{-1}(1/2)<0 \Rightarrow M_S > 0. \tag{53}$$

So relative intensification is southwards and $\mathbf{M}_S$ is eastwards.

For instance, with reference to Fig. 1, panels a and b:

$Q(\psi) = \psi \rightarrow Q^{-1}(1/2) = 1/2 \rightarrow M_N > M_S \rightarrow$ northward intensification,

$Q(\psi) = \psi + 1 \rightarrow Q^{-1}(1/2) = -1/2 \rightarrow M_S > M_N \rightarrow$ southward intensification.

Remark. Unlike the previous examples, if $Q(\psi)$ is a non-linear function and C is a constant, then, $Q^{-1}(1/2 - C) \neq Q^{-1}(1/2) - C)$. This means that, in general, the addition of a constant to the total vorticity does not transfer any intensification from one zonal boundary to the other.

The remaining possibility:

$$Q^{-1}(1/2)=0 \tag{54}$$

indicates a bifurcation at $y = 1/2$ that separates the domain into two regions like an impermeable wall, so that only the anti-symmetric transport can take place, as it does not occur through this wall, whatever the longitude. In fact, in each region, the total mass transport, e.g. $\mathbf{M}'_{tot} = \mathbf{M}'_{tot}\hat{\mathbf{i}}$ and $\mathbf{M}''_{tot} = \mathbf{M}''_{tot}\hat{\mathbf{i}}$, is separately zero:

$$M'_{tot} = \int_0^{1/2} u\,dy = -\psi_{\text{int}}(1/2) = 0, \;\; M''_{tot} = \int_{1/2}^{1} u\,dy = \psi_{\text{int}}(1/2) = 0$$

and each region hosts a full gyre. Conversely, the symmetric mass transport carries the fluid from edge to edge, and, therefore, it would not be compatible with Eq. 54. In conclusion:

$$Q^{-1}\left(1/2\right)=0\Rightarrow \mathbf{M}_S=\mathbf{M}_N. \tag{55}$$

For instance, in panel c of Fig. 1, $Q(\psi) = \psi + 1/2 \rightarrow Q^{-1}(1/2) = 0 \xrightarrow{(55)} \mathbf{M}_N = \mathbf{M}_S$.

To summarise, free modes governed by Eqs. 11 to 14 exhibit northward intensification if $Q^{-1}(1/2) > 0$, southward intensification if $Q^{-1}(1/2) < 0$ and same intensification in the north and south if $Q^{-1}(1/2) = 0$.

5. Some non-linear free modes in elongated basins and their intensification

Elongated basins allow a boundary layer approximation of the 2D solution in the proximity of the meridional boundaries, while in the remaining part of the domain, where the flow is basically zonal, the exact solution can be investigated in terms of an ordinary differential equation. The details are explained in the Appendix. Once $Q(\psi)$ is given, the problem lies in the integration of ordinary Eq. A3, with boundary conditions in Eq. A4. The asymmetric nature of the solution of the ordinary problem in Eqs. A3 and A4 is known from Eq. A5, while the localisation of the consequent intensified transport is determined *a priori* on the basis of Eqs. 52, 53, and 55. Below three cases are analysed.

First,

$$Q\left(\psi\right)=\tan^{-1}\left(\psi\right). \tag{56}$$

Given that $Q_\psi = (1 + \psi^2)^{-1}$, the choice in Eq. 56 satisfies inequality in Eq. 13. Moreover, $Q^{-1}(1/2) = \tan(1/2) > 0$, so criterion in Eq. 52 applies and relative intensification is northwards with $\mathbf{M}_N$ pointing east. The projection of D_{int} on the y–axis lies in interval ($0 \le y < 0.67$). The solution of the problem in Eqs. A3 and A4, with Eq. 56, is plotted in panel a of Fig. 2. There, the asymmetry in Eq. 40, in favour of northward intensification, is evident. Panel b of the same figure

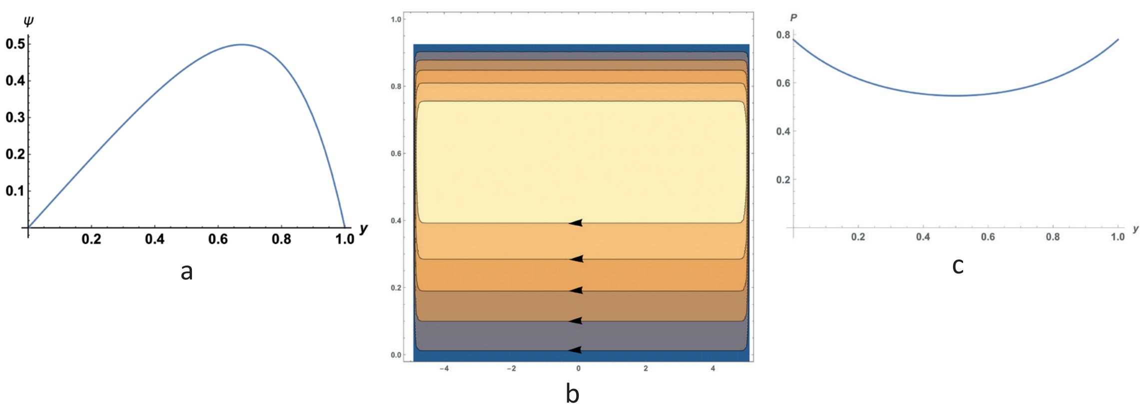

Fig. 2 - Panel a is the plot of the solution of the problem represented by Eqs. A3 and A4, that is $\psi(0, y)$. The streamlines of the full solution are represented in panel b. Panel c shows function $p(y)$ defined in Eq. 51.

shows the streamlines of the 2D solution crowded in the proximity of the northern boundary and dominant intensification with respect to the southern boundary. Panel c shows the plot of $p(y)$, which is positive in the full interval ($0 \le y \le 1$) and, hence, $y_1 = 1/2$.

Second,

$$Q(\psi) = \tan^{-1}(\psi) + 1/2. \tag{57}$$

The solution of the problem in Eqs. A3 and A4, with Eq. 57, is depicted in panel a of Fig. 3. The projection of D_{int} on the y–axis lies in interval ($0.2 < y < 0.8$). The position in Eq. 57, that trivially satisfies Eq. 13, is a special case of the kind:

$$Q(\psi) = F_{odd}(\psi) + 1/2 \tag{58}$$

where F_{odd} is any odd function of its argument. Eq. 58 implies:

$$Q^{-1}(y) = F_{odd}^{-1}(y - 1/2). \tag{59}$$

In turn, application of Eq. 59 to the first part of Eq. 50 yields:

$$M_N^s = -M_S^s = \frac{1}{2}\left[F_{odd}^{-1}(Y - {}^1/_2) + F_{odd}^{-1}({}^1/_2 - Y)\right] = \frac{1}{2}\left[F_{odd}^{-1}(Y - {}^1/_2) - F_{odd}^{-1}(Y - {}^1/_2)\right] = 0$$

and, therefore, $M_N = M_N^a = M_S^a = M_S > 0$. In conclusion, $M_N = M_S$, that is, both of them point east with the same intensity, according to criterion in Eq. 55. Panel b of Fig. 3 exhibits the circulation pattern of the mode with Eq. 57, and represents a special case of a more general, but fairly similar, mode solution with Eq. 58 in place of Eq. 57. Panel c presents the plot of $p(y)$ keeping in mind that, in the present case, the functional dependence of Q^{-1} on its argument is not y but $y - 1/2$.

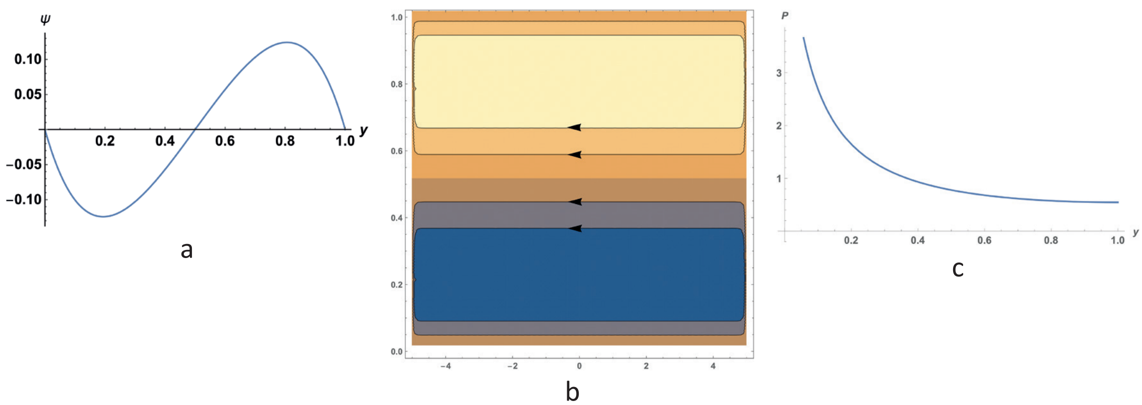

Fig. 3 - Panel a is the plot of the solution of the problem in Eqs. A3 and A4, that is $\psi(0, y)$. The streamlines of the full solution are represented in panel b. Panel c shows function $p(y - 1/2)$.

Third,

$$Q(\psi) = \exp(\psi). \quad (60)$$

The solution of the problem in Eqs. A3 and A4, with Eq. 57, is found in panel a of Fig. 4. The functional relationship in Eq. 60 also satisfies Eq. 13. The asymmetry in Eq. 40 is in favour of southward intensification, with $\mathbf{M}_N$ pointing east, as confirmed by inequality $Q^{-1}(1/2) = ln(1/2) < 0$, in accordance with criterion in Eq. 53. The projection of D_{int} on the y–axis lies in the interval ($0.33 < y \leq 1$). Panel b of Fig. 4 shows the streamlines of the 2D solution crowded in the proximity of the southern boundary.

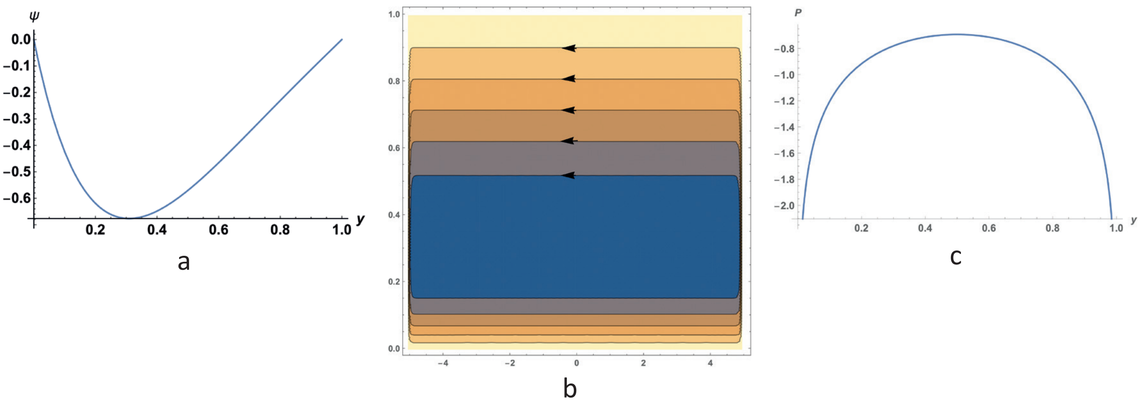

Fig. 4 - Panel a is the plot of the solution of the problem in Eqs. A3 and A4, that is $\psi(0, y)$. The streamlines of the full solution are represented in panel b. Panel c shows function $p(y)$ defined in Eq. 51, which is negative in the full interval ($0 < y < 1$) and, hence, $y_2 < 1/2$.

6. Conclusions

By reason of Eq. 12, all the solutions of the problem in Eqs. 11 to 14 are zonal, apart from small border regions in which the circulation patterns bend over to close the streamlines. In other words, they are not very sensitive to a different $Q(\psi)$. In this perspective, the latitude of the intensified transport seems to be the unique feature that distinguishes classes of solutions.

Acknowledgments. The authors thank an anonymous referee for quoting the paper of Bouchet and Venaille.

REFERENCES

Blumen W.; 1968: *On the stability of quasi-geostrophic flow*. J. Atmos. Sci., 25, 929-931.

Bouchet F. and Venaille A.; 2012: *Statistical mechanics of two-dimensional and geophysical flows*. Phys. Rep., 515, 227-295.

Crisciani F. and Badin G.; 2014: *A note on the symmetric and anti-symmetric constituents of weakly non-linear solutions of classical wind-driven ocean circulation models*. Eur. Phys. J. Plus, 129, 142, 12 pp., doi: 10.1140/epjp/i2014-14142-y.

Crisciani F. and Mosetti R.; 2021: *Remarks on the westward intensification of wind-driven ocean transport*. Bull. Geoph. Ocean., 62, 577-594.

Crisciani F. and Mosetti R.; 2022: *Ierley's regional model of wind-driven circulation: a tool to prove that intensification is westward*. Bull. Geoph. Ocean., 63, 519-534.

Fofonoff N.P.; 1954: *Steady flow in a frictionless homogeneous ocean*. J. Mar. Res., 13, 254-262.

Greenspan H.P.; 1962: *A criterion for the existence of inertial boundary layers in the oceanic circulation*. Proc. Natl. Acad. Sci. U.S.A., 48, 2034-2039, doi: 10.1073/pnas.48.12.2034.

Hendershott M.C.; 1987: *Single layer models of the general circulation*. In: H.D.I. Abarbanel and W.R. Young (eds), General circulation of the ocean, Springer-Verlag, Berlin, Germany, 291 pp.

Krauss W.; 1973: *Methos and results of theoretical oceanography. Dynamics of the homogeneous and quasi homogeneous ocean, vol. 1*. Gebruder Borntraeger, Berlin-Stuttgart, Germany, 302 pp.

Moro B.; 1987: *On the inertial motion of a homogeneous ocean*. Dyn. Atmos. Oceans, 11, 1-17, doi: 10.1016/0377-0265(87)90011-X.

Pedlosky J.; 1987: *Geophysical fluid dynamics*. Springer-Verlag, Berlin, Germany, 710 pp.

Pedlosky J.; 1996: *Ocean circulation theory*. Springer-Verlag, Berlin, Germany, 453 pp.

Pedlosky J.; 2016: *Fofonoff negative modes*. Fluids 2016, 1, 13, 11 pp., doi: 10.3390/fluids1020013 .

Vallis G.K.; 2006: *Atmospheric and oceanic fluid dynamics*. Cambridge University Press, Cambridge, UK, 745 pp.

Corresponding author: Renzo Mosetti
E-mail: rmosetti@gmail.com

Appendix: Approximations involving Eq. 11 and its integration in elongated basins

Elongated basins exhibit different horizontal length scales:

$$\begin{aligned} x &= \lambda L x' \\ y &= L y' \end{aligned} \tag{A1}$$

where λ is a dimensionless constant such that, in the model under investigation, λ^{-2} is very small in a sense that is clarified in what follows. In Eq. A1, the apex provisionally refers to dimensionless variables. The dimensional version of Eq. 8 is:

$$\frac{1}{\rho f_0}\nabla^2 p + \beta_0 y = Q_*\left(p\right)$$

where $p = \rho f_0 UL\psi$ is the perturbation pressure at the geostrophic level, $\beta_0 = U\beta / L^2$ is the planetary vorticity gradient, and $Q_* = \beta_0 LQ'$ is the total vorticity. After some trivial rearrangements and deletion of quotes, the dimensionless version is:

$$\lambda^{-2}\frac{\partial^2\psi}{\partial x^2} + \frac{\partial^2\psi}{\partial y^2} + \beta y = \beta Q\left(\psi\right). \tag{A2}$$

Far enough from the meridional boundaries, where the streamlines bend over to close themselves and $\partial^2\psi / \partial x^2 >> 1$, the order of magnitude of the first term of Eq. A2 is significantly smaller than that of the others. To the extent that λ^{-2} can be considered negligibly small compared to the unit, Eq. A2 becomes the ordinary equation:

$$\left(\delta_I / L\right)^2 \Psi_{yy} + y = Q\left(\Psi\right) \tag{A3}$$

with boundary conditions:

$$\Psi\left(0\right) = \Psi\left(1\right) = 0. \tag{A4}$$

As in section 2, in Eq. A3 $\beta^{-1} = (\delta_I / L)^2$ has been replaced. In the case of Eq. A3, Eq. 40 takes the form:

$$\Psi\left(1/2 - y\right) \neq \Psi\left(1/2 + y\right). \tag{A5}$$

The full 2D-model and the situation in the proximity of western boundary $x = -\lambda$, where a boundary layer approximation of the solution can be introduced, is now taken into consideration. Considering:

$$\eta = \left(L / \delta_I\right)\left(x + \lambda\right) \tag{A6}$$

as the boundary layer coordinate, and:

$$\phi_W = \phi_W\left(\eta, y\right) \tag{A7}$$

as the related correction to be added to $\Psi(y)$ to satisfy Eq. 14 in $x = -\lambda$, then:

$$\left(\delta_I / L\right)^2 \left(\nabla^2\phi_W + \nabla^2\Psi\right) + y = Q\left(\phi_W + \Psi\right). \tag{A8}$$

Noting that $(\delta_I/L)^2\nabla^2\phi_W \approx \frac{\partial^2\phi_W}{\partial\eta^2}$ and $(\delta_I/L)^2\nabla^2\Psi = Q(\Psi) - y$, Eq. A8 takes the form $\frac{\partial^2\phi_W}{\partial\eta^2} = Q(\phi_W + \Psi) - Q(\Psi)$. Within the validity of truncated Taylor expansion $Q(\Psi + \phi_W) \approx Q(\Psi) + Q_\psi\phi_W$, the equation for ϕ_W becomes:

$$\frac{\partial^2\phi_W}{\partial\eta^2} = Q_\Psi\phi_W. \tag{A9}$$

The asymptotic and boundary conditions to be prescribed to the general integral of Eq. A9 are:

$$\phi_W\left(+\infty, y\right) = 0 \tag{A10}$$

$$\phi_W\left(0, y\right) + \Psi\left(y\right) = 0. \tag{A11}$$

The solution of the problem, in Eqs. A9 to A11, is:

$$\phi_W(\eta, y) = -\Psi(y) exp\left(-\sqrt{Q_\Psi}\eta\right) \quad \text{(A12)}$$

Thus, in the western and central regions of the domain, the solution is

$$\psi_W\left(x,y\right) = \Psi\left(y\right)\left\{1-\exp\left[-\sqrt{Q_\Psi}\ L\left(x+\lambda\right)/\delta_I\right]\right\}. \quad \text{(A13)}$$

Quite analogously, in the eastern and central regions, the solution is:

$$\psi_E\left(x,y\right) = \Psi\left(y\right)\left\{1-\exp\left[\sqrt{Q_\Psi}\ L\left(x-\lambda\right)/\delta_I\right]\right\}. \quad \text{(A14)}$$

An overall view of the streamlines can be obtained by means of the composite form:

$$\psi\left(x,y\right) = \Psi\left(y\right)\left\{1-\exp\left[-\sqrt{Q_\Psi}\ L\left(x+\lambda\right)/\delta_I\right]\right\}\left\{1-\exp\left[\sqrt{Q_\Psi}\ L\left(x-\lambda\right)/\delta_I\right]\right\}. \quad \text{(A15)}$$

Once the problem in Eqs. A3 and A4 is solved, Q_ψ becomes a known function of y and Eq. A15 is singled out.